Dmytro Demirskyi, Hossein Sepehri-Amin, Oleg O. Vasylkiv, "**High-temperature deformation and consolidation of polycrystalline α-SiC by spark plasma sintering.**" ***Int J Appl Ceram Technol*** (2024); e14967 https://doi.org/10.1111/ijac.14967

Supplementary information

S.1 Details on the experiments carried out to optimize processing.

In this research, we utilized the Design of Experiments (DoE) technique to investigate the relationship between processing parameters and the response of a specified experimental output variable, operating under the assumption of a direct correlation between these factors. The experimental configuration employed for the optimization of Spark Plasma Sintering (SPS) processing of silicon carbide bulks, with a focus on relative density as the output variable, is outlined in **Table S1**.

Table S1: The design of the experiment for the consolidation of alpha silicon carbide

SPS run ID	Temperature, °C	Dwell at T°C, min	*x1*	*x2*	Yield (Density, %)
1	1960	20	-1	-1	91.2
2	2080	20	1	-1	91.7
3	1960	40	-1	1	90.1
4	2080	40	1	1	93.4
5	1960	20	-1	-1	92.6
6	2080	20	1	-1	97.9
7	1960	40	-1	1	89.7
8	2080	40	1	1	96.7
9	2020	30	0	0	99.7
10	2020	30	0	0	99.8
11	2093	30	1.215	0	94.2
12	1947	30	-1.215	0	91.5
13	2020	30	0	1.215	96.5
14	2020	42	0	-1.215	99.9
15	2020	18	0	0	99.4
16	2020	30	0	0	99.5
17	1990	37	-0.5	0.7	92.3
18	2050	37	0.5	0.7	94.5
19	1950	33	0.5	1.3	96.7
20	2050	33	0.5	1.3	96.3
21	2020	40	0	1	98.6
22	2020	40	0	1	99.5

S.2 XRD phase analysis

X-ray diffraction (XRD) phase analysis was conducted on the initial powder material, revealing the presence of a single-phase alpha silicon carbide with a 6H-polytype structure possessing a space group of 186 and lattice parameters a = 3.085(8) Å and c = 15.140(4) Å. The crystallite size was determined to be in the range of 22–28 nm, indicating that the powder consisted of aggregates comprising approximately 20 crystallites, with a surface area exceeding 10 m^2/g.
Subsequent XRD analysis of the silicon carbide ceramics produced through SPS revealed a two-phase composition characterized by the presence of 6H and 15R-polytypes (**Fig. S2**). Upon consolidation above 2000 °C, the crystallite size of the 6H-polytype increased to over 230 nm from the initial powder size of 22-28 nm. The proportion of the 15R-phase varied significantly depending on the specific processing conditions utilized (**Fig S3**).
The XRD data from this study indicated that the specimens examined did not exhibit any phases other than the 6H or 15R polytypes. While the transformation sequence for alpha silicon carbide is conventionally understood to progress from 6H to 15R and then to 4H [1,2], limited studies were focused on the processing and characterization of additive-free α-SiC ceramics [3]. It is plausible that impurities or additives introduced during the consolidation process may influence the transformation behavior of silicon carbide.

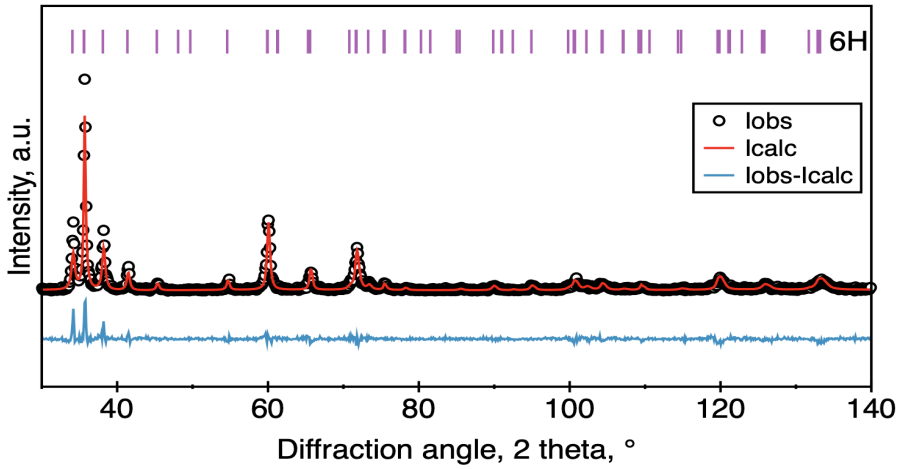

Figure S1: X-ray diffraction pattern observed for raw silicon carbide powder. Vertical lines indicate the Bragg position for the 6H silicon carbide phase. Red solid line shows the refinement performed using the Rietveld method.

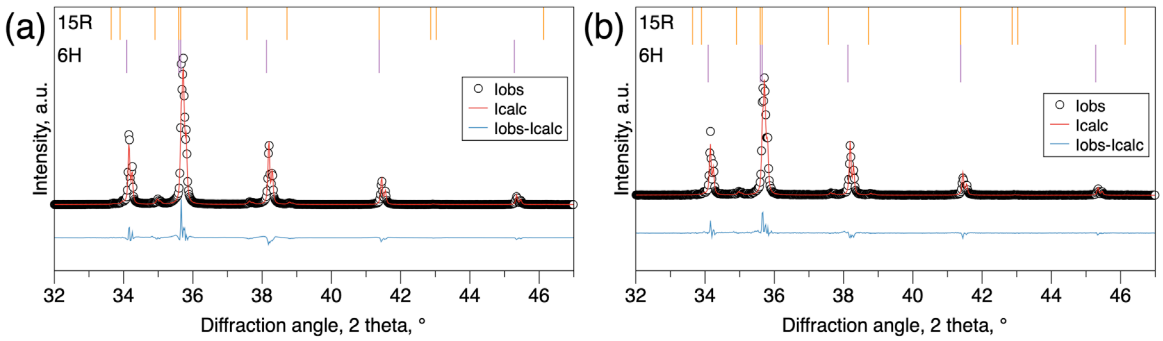

Figure S2: Typical X-ray diffraction pattern observed after the SPS consolidation using the (a) 2010/20 configuration and (b) 2050/48 configuration. Vertical lines indicate the Bragg

position for the 6H and 15R silicon carbide phases. The red solid line shows the refinement performed using the Rietveld method. Note a slight difference in the intensity of the 15R peaks. The weight fraction of the 15R silicon carbide polytype was 7.1±0.1 and 5.8±0.1 for (a) and (b), respectively.

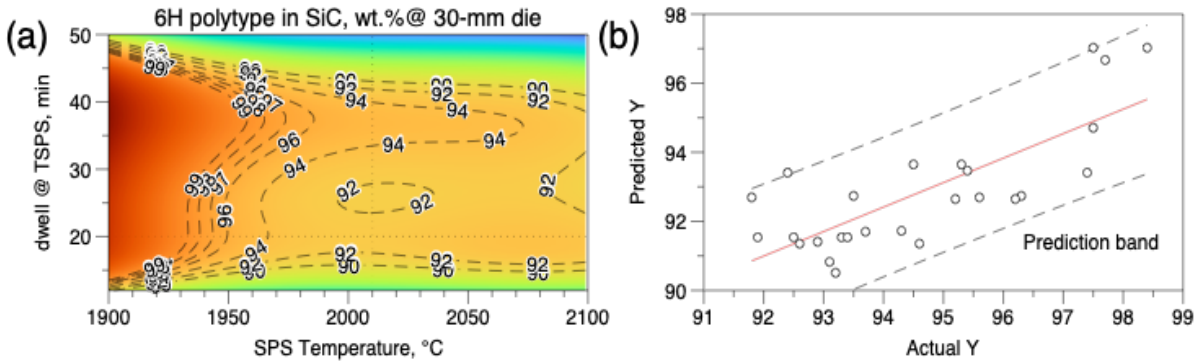

Figure S3: Response surface representation of the weight content of the 6H SiC polytype in the SPSed silicon carbide ceramics. The dotted lines show the 2010/20 configuration. (b) compares the actual value of the 6H polytype in SiC vs predicted using a linear regression.

S.3 Hardness data

The silicon carbide that contained no additives exhibited notably high hardness, measured at approximately 31.7±1.1 GPa under a load of 49 N. An increase in the applied load resulted in a modest reduction in hardness; specifically, at loads of 96 N and 196 N, the hardness values recorded were 28.3±0.2 GPa. **Figure S4** illustrates representative scanning electron microscopy (SEM) images at both low and high magnification of the indents, which were employed to validate the data obtained through optical microscopy (OM) measurements conducted immediately following the indentations. It is important to note that the maximum unforced error observed between OM and SEM measurements was approximately 8%. The overall hardness is influenced by factors such as load, density, and grain size. For a given load, the relationship between hardness, density, and grain size can be described as a nonlinear function, as illustrated in **Figure S5**.

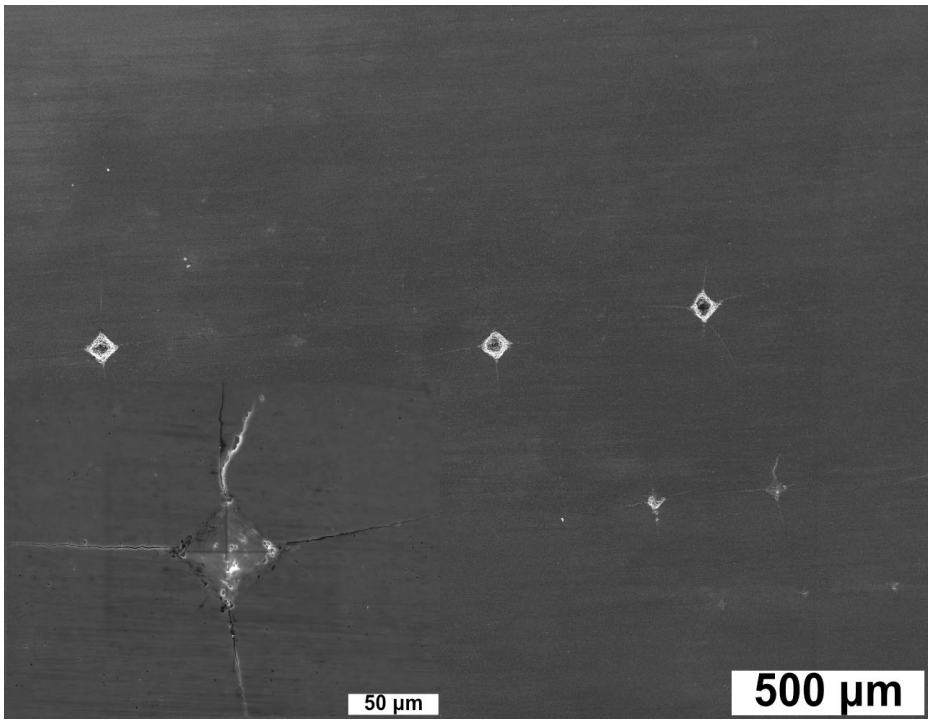

Figure S4: Representative scanning electron microscopy (SEM) images of silicon carbide bulk samples were captured utilizing 49N and 98N loads to validate the initial hardness measurements acquired through optical microscopy.

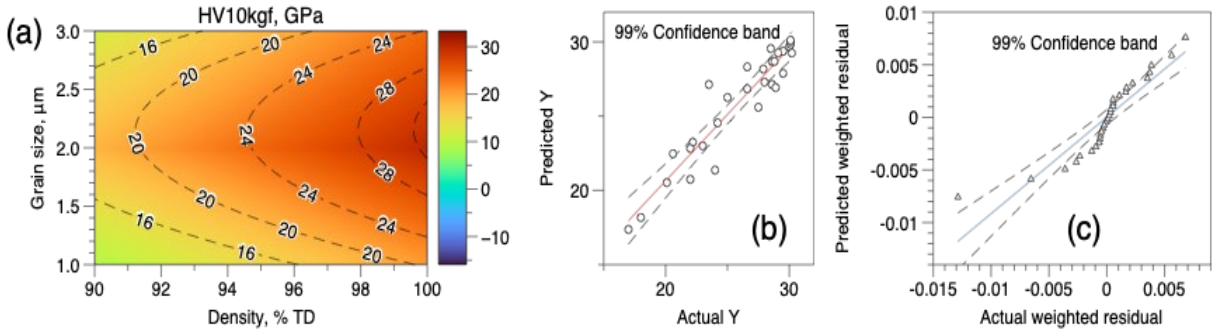

Figure S5: Response surface model depicting the hardness of silicon carbide ceramics as a function of both density and grain size. These silicon carbide specimens were sintered using a 30-mm die and pressure of 45 MPa using OY-–15 powder.

S.4 Data used for the construction of the deformation maps

The flexural strength's sensitivity can be explained by the relationship between applied strain rate and resulting deformation. This method for deformation maps was developed by Frost-Ashby [4]. This includes a calculation of the theoretical rate using rate equations for various mechanisms such as low-temperature plasticity, dislocation creep (power law creep), diffusion creep (controlled by volume diffusion or grain-boundary diffusion), grain-boundary sliding, etc. [4]. These mechanisms are associated with deformation, and the principal equation utilized

is given as

$$\dot{\varepsilon} = \mathrm{A} \cdot \frac{\Omega}{\mathbf{b^3}} \cdot \frac{\mu \mathbf{b}}{kT} \cdot \left(\frac{\mathbf{b}}{d}\right)^p \cdot \left(\frac{\sigma}{\mu}\right)^n \cdot D \quad \text{(eq. S1)}$$

Where $\dot{\varepsilon}$ is rate, A represents a constant, *d* indicates grain size, Q is the activation energy, R denotes the gas constant, T signifies temperature in Kelvin, and *n* and *p* are the exponents corresponding to stress and grain size, respectively. Ω is atomic volume, and D is the diffusivity calculated as $D = D_0 \exp(-Q/RT)$. μ is the shear modulus calculated as $\mu = \mu_0 - d\mu \cdot T$ (μ_0 and dμ are shear modulus at 300 K and coefficient for dependence of shear modulus). **b** is the Burgers vector, while σ is the applied pressure.
The data in **Table S2**, gathered from refs [1, 4–6], was used to create these maps. There was no creep deformation data available for alpha silicon carbide at temperatures above 1600 °C, so the data used for creep analysis was from low-temperature studies, similar to the suggestions in [4, 5]. All calculations were done with a custom script in Matlab / Octave. As suggested in [4], sometimes the rate observed in the field is actually specific to one mechanism, rather than a combination of all active mechanisms. Chosen strain rate fields indicated with dash lines: 1, 1×10^{-4}; 1×10^{-8}; 1×10^{-12}; 1×10^{-16}.

Table S2: Data used for the construction / calculation of the deformation maps of alpha silicon carbide

Property / Parameter	Value	Units
Atomic volume	$2.07\cdot10^{-29}$	m^3
Burgers vector, 1/3 <11-20>	$1.78\cdot10^{-10}$	m
Shear modulus at 300 K	$2\cdot10^5$	MPa
Dependence of shear modulus	-0.18	a.u.
Lattice diffusion pre-exponential	$8.4\cdot10^5$	m^2/s
Lattice diffusion activation energy	912	kJ/mol
Bondary diffusion pre-expontial	$3.1\cdot10^{-7}$	m^3/s
Boundary diffusion activation energy	611	kJ/mol
Dislocation creep, exponent	5	a.u.
Dislocation creep pre-exponential factor	$2\cdot10^4$	MPa/m
Dislocation creep activation energy	912	kJ/mol
Low-temperature plasticity pre-exponential factor	$1\cdot10^9$	s^{-1}
Low-temperature plasticity stress exponent	2	a.u.
Low-temperature plasticity activation energy	912	kJ/mol
Poison ratio	0.27	a.u.
Peierls stress	$11.5\cdot10^3$	MPa

S5. Flexural strength of SiC sample at 2000 °C.

Flexural strength of 2.08 GPa was achieved by silicon carbide bulk tested at 2000 °C under a 2.5 mm/min loading rate.

Title

Key Word		Product Name	
Test File Name	SiC1-D-2000-2.5mmmin.xtak	Method File Name	3point16mm.xmak
Report Date	2021/06/23	Test Date	2021/06/23
Test Mode	Single	Test Type	3 Point Bend
Speed	0.5mm/min	Shape	Plate
No of Batches:	1	Qty/Batch:	1

Name Parameters Unit	Max_Force Calc. at Entire Areas N	Max_Stress Calc. at Entire Areas MPa
SiC1-D-2000	1624.70	2079.62

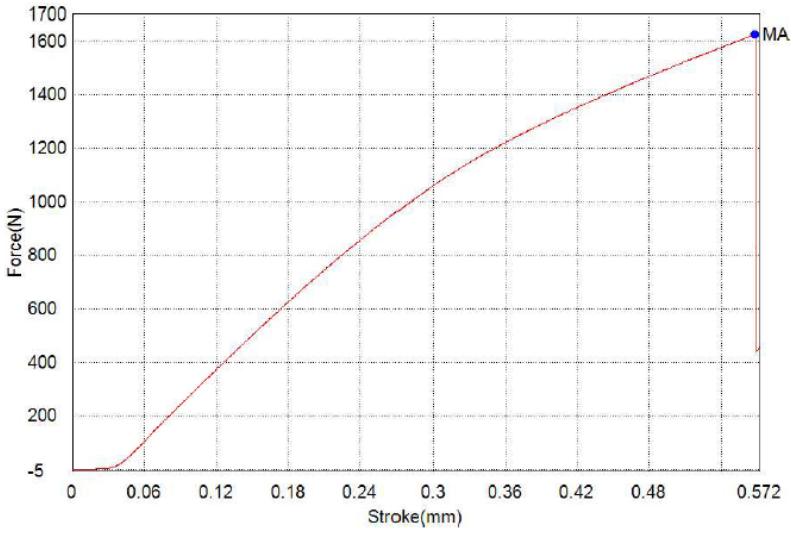

Comment

[1] R.A. Andrievski, I.I. Spivak, Strength of Refractory Compounds. Metallurgiya, Chelyabinsk, 1989. [in Russian].
[2] R. Stevens, Defects in silicon carbide. J. Mater. Sci. 7 (1972) 517–521. doi: https://doi.org/10.1007/BF00761949.
[3] J.M. Bind, J.V. Biggers, Hot-Pressing of Silicon Carbide with 1% Boron Carbide Addition, J. Am. Ceram. Soc. 58[7-8] (1975) 304–306. doi: https://doi.org/10.1111/j.1151-2916.1975.tb11482.x.
[4] H.J. Frost, M.F. Ashby, Deformation-Mechanism Maps: The Plasticity and Creep of Metals and Ceramics, Pargamon Press, Oxford, 1982.
[5] P.M. Sargent, M.F. Ashby, Deformation-Mechanism Maps for SiC, Scr. Metall. 17[7] (1983) 951–957.
[6] T.Ya. Kosolapova, T.V. Andreeva, T.S. Bartnitskaya et al., Non-metallic refractory compounds. Metallurgiya, Moscow, 1985. [in Russian].